

# Intelligent Workpiece Setup in Micro pattern-Machining on a Large Surface

J.-S. Kim<sup>1</sup>, M.-Y. Yang<sup>1</sup>, J.-G. Choi<sup>2</sup>

<sup>1</sup>Agile Technology Lab, Dept. of Mechanical engineering, KAIST 373-1,  
Guseong-dong, Yuseong-gu, Daejeon, 305-701, South Korea

<sup>2</sup>Dept. of Automotive Engineering, Suncheon National University,  
315 Maegok, Suncheon, Jeonnam 540-742, South Korea

## Abstract

In micro pattern machining on a large surface such as that on a LCD (Liquid Crystal Display) product, a workpiece setup is a difficult task as a high level of stiffness is required for a setup device for a heavy and a large workpiece. In this study, a new type of a 3-DOF (Z-translation, Pitch, Roll motion) precision tilt stage for a heavy load and large-surfaced workpiece setup is developed. The workpiece setup can be compensated by the tilting stage with the reference of the relative distance of the tool and a workpiece with closed-loop positioning control.

## Keywords:

Ultra –precision, Modeling, Compensation

## 1 INTRODUCTION

In micro-pattern machining on a large surface such as that for a LCD (Liquid Crystal Display) product, workpiece setup is a difficult task because a high level of stiffness is required for the setup device for a heavy and large workpiece.

Because micro-pattern machining on a large surface is a process that requires more than one day for completion, a workpiece setup device must be sufficiently stiff. Moreover, the setup must be adhere to sub-micron position accuracy.

Therefore, the stiffness of a setup device and precise positioning control are important factors in this process.

Workpiece setup in micro-pattern machining is also a very important process, as the flatness of the mold surface directly affects the final injection molding product.

What is needed is a nano-precise positioning control and a compensation technology that takes into account the heavy load and a large surface of the workpiece in order to improve the quality of the final product and to reduce the setting process time.

X, Y, Z-translation and the pitch, roll, yaw-motion errors can occur during workpiece setup.

During workpiece setup, the process errors of the X, Y-translation error and yaw-motion error are compensable using precision-machine X, Y-axis bed and a C-axis rotation bed respectively.

The remaining errors that are not compensable generally by the machine itself are the target values. Offsetting these errors is a challenge, but hard to compensate and also critical to micro-pattern mold on a large surface.

Therefore, in this study, a new type of a precise tilt with 3-DOF (Z-translation, Pitch, Roll motion) stage for a heavy load and large-surfaced workpiece setup is developed.

The tilt stage compensates the flatness of the workpiece precisely with measured data regarding the relative distance of tool and workpiece.

Maximum load capacity	200kg
Height of the tilt stage	under 100mm

Width of the tilt stage	400x400(mm)
Working distance	Over 100 $\mu$ m
Resolution	0.05 $\mu$ m
Repeatability	0.1 $\mu$ m

Table 1: Tilt stage design specification

The design specification of the tilt stage is decided by a target process progresses with a 400x400(mm) workpiece and is machined in less than 20 $\mu$ m micro-patterns within a 0.5 $\mu$ m machined precision.

The tilt stage uses piezo actuators and flexible guides to create the precision motions. The structure of the system is designed considering the stiffness and amplification of the moving range in order to hold a heavy load and to increase working distance. In general, an amplification mechanism causes the system to be weak and complex. In this system, compactness and the stiffness of tilt stage are focused upon.

## 2 DESIGN OF SYSTEM

The system is constructed with a three-axis actuating system, as shown in Figure 1.

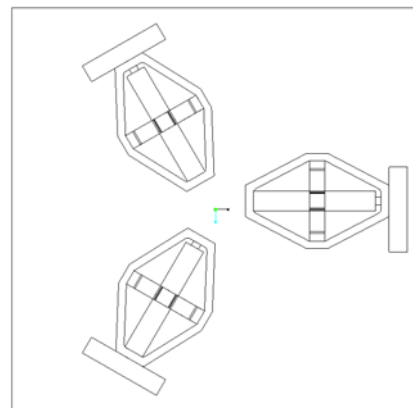


Figure 1: Configuration of the tilt stage

The actuating system is composed of an inclined bridge and standing half bridge, as shown in Figure 2.

A piezo actuator is placed inside of the inclined bridge; between the gaps of the inclined bridge the standing half bridge is located.

The workpiece is loaded onto the upper side of the half bridge and the load is transmitted inside of the inclined bridge and to the piezo actuator.

The piezo actuator is generally strong in terms of the compressive force but weak in terms of the tensile force.

By considering the characteristics of the piezo actuator, the piezo actuator is always applied compressive force when the workpiece is loaded onto the upper side of the half bridge in the structure of this system.

The piezo actuator actuates a displacement drive by means of voltage control. As the length of the piezo actuator is expanded by the positive voltage, the upper side of the half bridge moves to above. Against this action, the length of the piezo actuator is decreased by the negative voltage, and the upper side of half bridge moves to down.

During this process, the workpiece is loaded onto the acting system and compressive force is applied in the direction of the length of the piezo actuator. Hence there is no gap between the piezo actuator and flexible guide.

The structure of the tilt stage is designed using this concept. This system can hold its stiffness and uses a ball contact between the piezo actuator and the flexible guide.

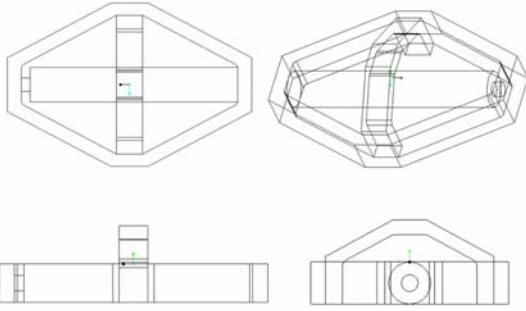


Figure 2: Configuration of actuating system

Figure 3 shows the force transmission of guide as the workpiece is loaded onto the actuating system. The compressive force on the piezo actuator ( $F_k$ ) by the workpiece load force ( $F_L$ ) can be obtained by a force transmission calculation. Thus, the minimum actuating force of the piezo actuator can be obtained.

Moreover, a deformation modeling equation is set by the workpiece load and piezo actuator force to satisfy the desired amplification.

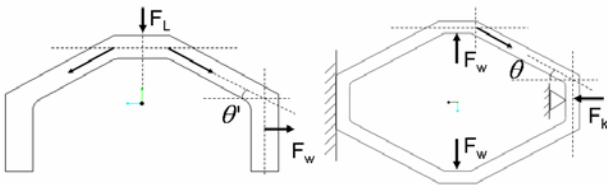


Figure 3: Force transmission by a workpiece

$$F_w = \frac{F_L}{2 \tan \theta'} \quad (1)$$

$$F_k = \frac{F_L}{2 \tan \theta' \cdot \tan \theta} \quad (2)$$

Figure 4 shows deformation of the guide by the workpiece load and piezo actuator force.

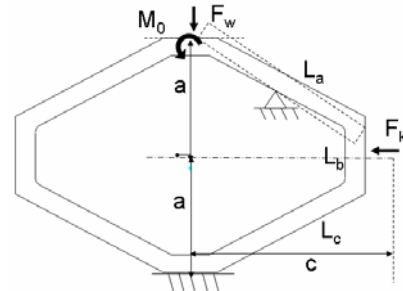


Figure 4: Applied force in the actuating system

1.  $F_w$  = Workpiece load
2.  $M_o$  = Moment of mount
3.  $F_k$  = Actuating force of the piezo actuator
4.  $L_a, L_b, L_c$  = Length of each guide

The deformation equation is expressed using castigliano's theorems to obtain the deformation in the desired direction.

The equation is written below in consideration of  $L_a$ .

$$M_a = M_o - F_w \cos \theta \cdot x$$

$$\delta a = \int \left( \frac{M_a}{EI} \right) \left( \frac{\partial M_a}{\partial F_w \cos \theta} \right) dx \quad (3)$$

$$M_a = M_o - F_k \sin \theta \cdot x$$

$$\delta a' = \int \left( \frac{M_a}{EI} \right) \left( \frac{\partial M_a}{\partial F_k \sin \theta} \right) dx \quad (4)$$

The equation is written below in consideration of  $L_b$ .

$$M_b = M_o - F_w \tan \theta \cdot y$$

$$\delta b = \int \left( \frac{M_b}{EI} \right) \left( \frac{\partial M_b}{\partial F_w \tan \theta} \right) dy \quad (5)$$

$$M_b = M_o - F_k \cdot y$$

$$\delta b' = \int \left( \frac{M_b}{EI} \right) \left( \frac{\partial M_b}{\partial F_k} \right) dy \quad (6)$$

The equation is written below in consideration of  $L_c$ .

$$M_c = M_o - F_w \cos \theta \cdot x$$

$$\delta c = \int \left( \frac{M_c}{EI} \right) \left( \frac{\partial M_c}{\partial F_w \cos \theta} \right) dx \quad (7)$$

$$M_c = M_o - F_k \cos \theta \cdot x$$

$$\delta c' = \int \left( \frac{M_c}{EI} \right) \left( \frac{\partial M_c}{\partial F_k \cos \theta} \right) dx \quad (8)$$

The coordinate of each equation is set perpendicularly to each guide. The guide deformation equation of the desired direction is shown below.

$$\begin{aligned} \delta a &= \int_0^{\frac{L}{2}} \left( \frac{M_a}{EI} \right) \left( \frac{\partial M_a}{\partial F_k \sin \theta} \right) dx - \int_0^{\frac{L}{2}} \left( \frac{M_a'}{EI} \right) \left( \frac{\partial M_a'}{\partial F_w \cos \theta} \right) dx \\ &= \int_0^{\frac{L}{2}} \left( \frac{F_k \sin \theta \cdot x}{EI} \right) dx - \int_0^{\frac{L}{2}} \left( \frac{F_w \cos \theta \cdot x}{EI} \right) dx \\ &= \frac{L^3}{24E \left( \frac{bh^3}{12} \right)} (F_k \sin \theta - F_w \cos \theta) \end{aligned} \quad (9)$$

Table 2 shows the criterion for deciding unknown variables.

Length of piezo actuator	125mm
Working distance	120 $\mu$ m
F <sub>w</sub>	700N
Young's Modulus(E) of Guide material(AL6061-T6)	68947.6MPa
Amplification	2
Guide limitation of height	40mm

Table 2: limited conditions

In these conditions, the limitation of the height is decided considering the upper plate and bottom plate of the tilt stage.

Equation (9) can be applied to both the inclined bridge and the half bridge, as they are geometrically symmetric structures. Under limited conditions, unknown length variables are decided to design the tilt stage.

(mm)	Inclined bridge	(mm)	Half bridge
b	20	b'	15
h	7	h'	7
a	38.5	a'	16.5
c	72.5	c'	38.5
L	69.46	L'	37.34

Table 3: Decided variables

Young's modulus, as decided by the chosen variables and by the deformation, is checked with below equation.

$$\frac{3Eh}{2L^2} \cdot S_f \cdot \delta_{\max} \leq \sigma_{\text{yield}} \quad (10)$$

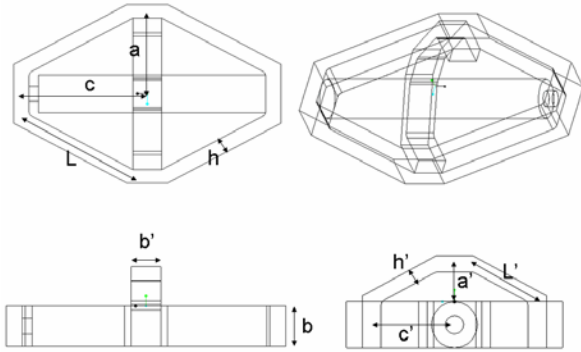


Figure 5: Decided variables of the guide

Each actuator is located in 100mm from the center to minimize any bending of the upper plate.

### 3 FEM ANALYSIS

To check the maximum stress of the system and the maximum z-axis moving range, FEM\_(Finite Element Method) analysis was carried out with design identical condition.

At first, the analysis condition with the maximum force generation of the piezo actuator and workpiece load is achieved in order to determine the minimum sufficient actuating condition. In addition, an analysis is carried out with displacement driven by the piezo actuator and workpiece load condition.

Figure 6 shows the stress distribution of the actuating system. The maximum stress is 159.7MPa, as applied at the corner of the half bridge. The yield stress of AL6061-

T6, as used in this system, is 240MPa. Thus, the maximum stress as applied to this system is less than the material yield stress. The amplified deformation to z-axis was found to be 180.3 $\mu$ m.

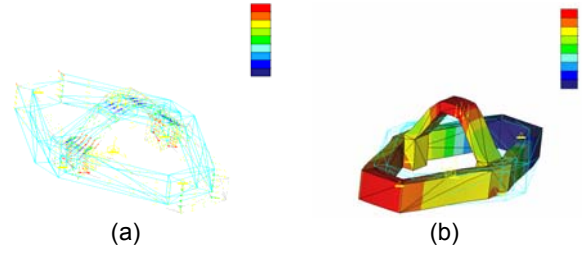


Figure 6: Maximum stress and Amplification

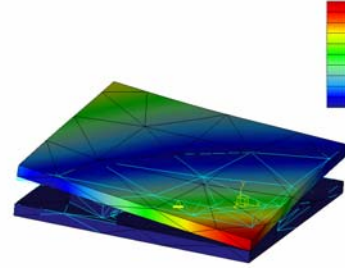


Figure 7: Mode analysis\_(natural frequency)

Through a mode analysis, the first-mode frequency of the system was determined to be 217.48Hz, with the second-mode 230.78Hz. The system is estimated to be adequately stiff compared to a general nano-stage and to actual machining conditions.

### 4 PERFORMANCE TEST OF TILT STAGE

A closed-loop stage movement test was performed by using P-gain control, as this system is designed for a setup application.

The total moving range and resolution of each axis were measured by a gap sensor and laser displacement sensor with the setting of a workpiece size of 400x400x100(mm).



Figure 8: Prototype of designed tilt stage

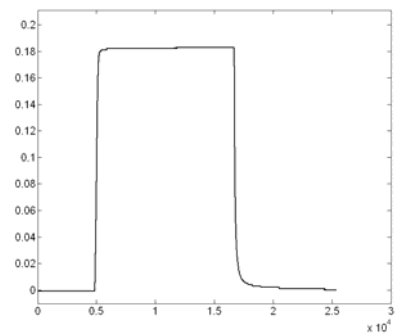


Figure 9: Maximum moving range

The maximum moving range was measured as 183 $\mu$ m. This is less than the desired amplified moving range. It is considered that material deformation around the bridge connection and screw deformation by load.

In addition, the 50nm-step movement was checked.

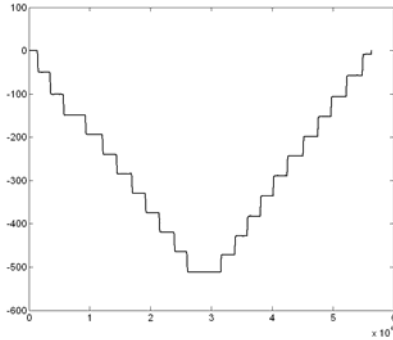


Figure 10: 50nm-step moving test

#### 4 WORKPIECE SETUP EXPERIMENT

A workpiece setup experiment was performed with a four-axis machine with a 400x400x100(mm) workpiece is loaded onto it.

With a laser sensor and a gap sensor, the relative distance of the tool and the workpiece were measured by setting the measuring sensor to the cutting tool position.

Generally the surface flatness process is achieved using an R-tool until a 10nm surface roughness is attained in micro-pattern machining over a large surface. The process for surface flatness is the shaping process with a short pitch by using a rounded R-tool.

The sensor measures the upper three points of the actuating system repeatedly to compensate the workpiece setup until the height of the three points is identical to the position accuracy.

By using this data, the tilt stage compensates the flatness of workpiece with the closed-loop positioning control.

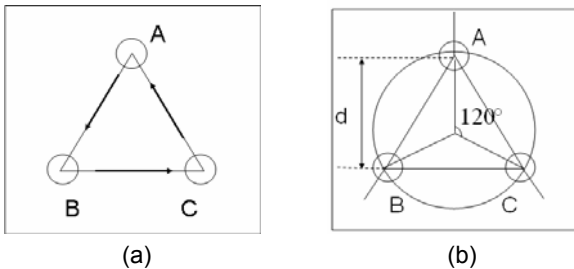


Figure 11: Measuring method and movement by position

1. A, B, C = movement of each actuator

$$2. \text{Pitch}_{\text{(roll)}} \text{ motion } \alpha = \frac{(A - (B + C) / 2)}{d} \quad (10)$$

$$3. \text{Z-translation motion } Z = \frac{(A + B + C)}{3} \quad (11)$$

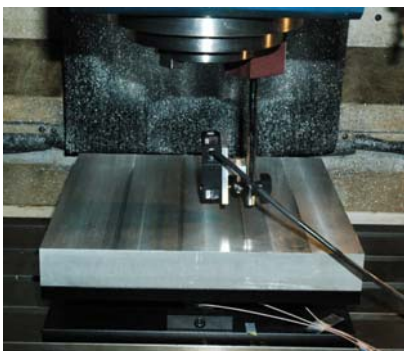


Figure 12: Workpiece setup experiment

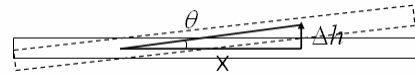


Figure 13: Tilting angle of compensation

$$\theta = \tan^{-1} \left( \frac{\Delta h}{x} \right) \quad (12)$$

Compensation angle is shown in equation (12).

$3.8 \times 10^{-5}$  degree compensated tilting angle was measured by tilt stage when actuating system moves 100nm. By the scanning of the workpiece surface, the compensation of setup was compared.

The accuracy of the setup is achieved within 0.5 $\mu$ m machined precision in three dimensions.

This workpiece setup process by using the tilt stage can be applied to micro-features machining on a large surface.

#### 5 SUMMARY

A novel 3-DOF (Z-translation, Pitch, Roll motion) precise tilt stage appropriate for a heavy load and a large surface workpiece setup was developed.

By using the tilting stage, improvement of a heavy workpiece setup could be confirmed with sub-micron accuracy over the entire large surface.

#### 6 ACKNOWLEDGMENTS

This work was accomplished as part of a core investigation project entitled the 'Development of intelligent technology for the manufacturing process of micro features on Large surface' of the Ministry of Commerce, Industry and Energy (MCIE) in Korea.

We extend our sincere thanks to our collaborators.

#### 7 REFERENCES

- [1] Elfizy, A.T., Bone, G.M., Elbestawi, M.A., 2005, Design and control of a dual-stage feed drive, *International Journal of Tools and Manufacture*, 45/2:153-165
- [2] Ryu, J.W., Lee, S.-Q., Gweon, D.-G., Kee, S.-M., 1999, Inverse kinematic modeling of a coupled flexure hinge mechanism, *Mechatronics*, 9/6:657-674
- [3] Lee, S.-Q., Gweon, D.-G., 2000, A new 3-DOF Z-tilts micropositioning system using electromagnetic actuators and air bearings, *Precision Engineering*, 24/1:24-31
- [4] Chang, S.H., Tseng, C.K., Chien, H.C., 1999, An ultra-precision XY  $\theta$  z piezo-micropositioner part I: design and analysis, *IEEE Transaction on Ultrasonics, Ferroelectrics, and Frequency Control*, 46/4:897-905
- [5] Juhas, L., Vujanic, A., Adamovic, N., Nagy, L., Borovac, B., 2001, A platform for micropositioning based on piezo legs, *Mechatronics*, 11/7:869-897
- [6] Gao, P., Swei, S., Yuan, Z., 1999, New piezoelectric precision micropositioning stage utilizing flexure hinge, *Nanotechnology*, 10/4:394-398
- [7] Kim, J.H., Kim, S.H., Kwak, Y.K., 2003, Optimization of a Piezoelectric Actuator using Bridge-Type Hinge Mechanism, *Journal of the Korea Society of Precision Engineering*, 20/2:168-175